Forest Ecology and Management 289 (2013) 219–233

Contents lists available at SciVerse ScienceDirect

Forest Ecology and Management

journal homepage: www.elsevier.com/locate/foreco

Developing a computerized approach for optimizing individual tree removal to efficiently reduce crown fire potential

Marco A. Contreras [a,*], Woodam Chung [b,1]

[a] Department of Forestry, College of Agriculture, University of Kentucky, 214 Thomas Poe Cooper Building (Office: 204), Lexington, KY 40546-0073, USA
[b] Department of Forest Management, College of Forestry and Conservation, University of Montana, Missoula, MT 59812, USA

ARTICLE INFO

Article history:
Received 8 September 2011
Received in revised form 24 September 2012
Accepted 26 September 2012
Available online 28 November 2012

Keywords:
Tree growth model
Skidding cost
Skid-trail network
Fire modeling and simulation
Thinning treatments

ABSTRACT

Thinning is a common silvicultural treatment being widely used to restore different types of overstocked forest stands in western U.S. because of its effect on changing fire behavior. Typically, thinning is applied at the stand level using prescriptions derived from sample plots that ignore variability in tree sizes and location within stands. Thinning prescriptions usually specify tree removal in terms of number of trees or basal area, resulting in a large number of cut-tree spatial patterns that meet the same prescription. However, the effect of each pattern on reducing crown fire potential can vary widely depending on the spatial distribution of leave-trees after treatment. Additionally, stand-level thinning prescriptions ignore cut-tree locations, which influence the economic efficiency of the thinning operations. Lastly, decisions on tree selection affect future competition levels of remaining trees, but the associated spatial and temporal effects on tree growth and crown fire potential over time are not considered in the development of thinning prescriptions. To address the limitations of current stand-level thinning practices, we designed a computerized approach to optimize individual tree removal and produce site specific thinning prescriptions that efficiently reduce crown fire potential. Based on stem map and tree attributes derived from light detection and ranging (LiDAR) technology and a distance-dependent individual tree growth model, current and future tree-level fuel connections between adjacent trees were predicted and used as measures of crown fire potential. The approach makes the spatial selection of cut- and leave-trees that most efficiently reduces crown fire initiation and propagation over time while ensuring cost efficiency of the thinning treatment. Application results on a forest stand in western Montana show that the optimal tree selection provided by the computerized approach can reduce crown fire potential more efficiently than current thinning practices represented by a manual selection of tree removal.

1. Introduction

High intensity wildfires have resulted in large financial, social, and environmental costs in western U.S. This trend is not likely to decline soon; some estimates suggest that more than 27 million ha of forestland in the western U.S. have departed significantly from natural wildland fire conditions and are at medium to high risk of catastrophic wildfires (Schmidt et al., 2002). In response to the continuing threat of severe wildfires, the National Fire Plan (USDA and USDI, 2001) and the Healthy Forest Restoration Act (2003) promoted restoring forest habitats and reducing the risk of wildfire on federal lands.

Thinning has been widely used for restoring different types of overstocked forest stands (O'Hara et al., 1994) because it can change stand structures and alter fire behavior (Graham et al., 1999, 2004; Agee and Skinner, 2005). Typically, thinning treatments are applied at the stand-level using prescriptions developed from field sample plots, and cut-trees are subjectively selected by forest practitioners according to given prescriptions. However, the efficiency and effectiveness of these stand-level thinning practices are hardly evaluated when applied for reducing crown fire potential due to the following reasons. First, it is difficult to estimate the effects of thinning on altering fire behavior within a stand using average stand attributes. Stand-level thinning prescriptions are designed to reduce the likelihood of crown fire initiation by increasing canopy base height, and reduce crown fire propagation by decreasing canopy bulk density (Keyes and O'Hara, 2002; Graetz et al., 2007). However, due to variability within stands, canopy base height is difficult to estimate and neither the lowest nor the average crown base height (measured on an individual tree) is likely to be representative of the stand as a whole (Scott and Reinhardt, 2001). Moreover, the calculation of canopy bulk density assumes canopy fuels are distributed uniformly throughout the

* Corresponding author. Tel.: +1 859 257 5666; fax: +1 853 323 1031.
E-mail addresses: marco.contreras@uky.edu (M.A. Contreras), woodam.chung@umontana.edu (W. Chung).
[1] Tel.: +1 406 243 6606.

0378-1127/$ - see front matter © 2012 Elsevier B.V. All rights reserved.
http://dx.doi.org/10.1016/j.foreco.2012.09.038

stand, which is unlikely the case even in stands with simple structures (Scott and Reinhardt, 2001). Secondly, current stand-level thinning prescriptions usually specify percentages of total tree removal or per size class in terms of number of trees or basal area (Graham et al., 1999; Agee and Skinner, 2005), resulting in a large number of spatial patterns of cut-trees that meet the same thinning prescription for a stand (Contreras, 2010). Individual foresters who select and mark cut-trees are unable to evaluate the effects of each pattern on reducing crown fire potential, which can vary widely depending on the resulting spatial distribution of remaining trees after treatment (Contreras, 2010). Thirdly, stand-level thinning prescriptions often ignore the location of cut-trees relative to extraction points (i.e., road side or log landings), and thus forest practitioners often pursue "easy" trees to extract as long as it meets the thinning prescription without considering the effects on altering fire behavior (Contreras, 2010; Contreras and Chung, 2011). Lastly, decisions on cut-tree selection also affect micro-conditions and competition levels of remaining trees, thus influencing tree growth and fire behavior within a stand over time (Pretzch et al., 2002; Skov et al., 2004). However, spatial and temporal effects of remaining trees on individual tree growth and crown fire potential over time have not been considered when developing thinning prescriptions (Contreras, 2010).

The limitations described above are mainly due to the lack of individual tree-level information available for development and evaluation of detailed, site-specific thinning prescriptions. However, LiDAR technology, which has been widely used in recent years to obtain individual tree locations and attributes (Maltamo et al., 2006; Packalén and Maltamo, 2006; Suratno et al., 2009), can be used to capture spatial variability of individual trees within a stand and produce stem maps and tree attributes. To address the limitations of current stand-level thinning practices, we designed a computerized approach to optimize the selection of tree removal for an individual stand that can most efficiently reduce the susceptibility to high intensity crown fires over time while ensuring the economic efficiency of thinning operations. Using LiDAR-derived stem map and tree attributes, we characterized fuels by quantifying fuel connections among individual trees and made a spatial selection of cut- and leave-trees to reduce the risk of crown fire initiation and propagation to and through the stand canopy. Our approach design includes four functional modules for: (1) quantifying vertical and horizontal fuel connectivity of individual trees in a stand, (2) predicting individual tree growth over time using a distance-dependent growth model, (3) estimating location-specific costs of timber harvesting for individual trees, and (4) optimizing selection of cut-trees to maximize and maintain discontinuities in fuel connectivity over time while ensuring cost efficiency. We applied our computerized approach to a 4.6-ha forest stand located in the University of Montana's Lubrecht Experimental Forest (LEF) in western Montana. We considered an initial thinning prescription that removed all trees with diameter at breast height less than 12.5 cm (5 in.). Cut- and leave-tree selection was then optimized for the remaining trees to meet a target tree density of 300 leave-trees per ha after the initial thinning prescription.

2. Methods

2.1. LiDAR-derived stem map and tree attributes

In this study, we used LiDAR data acquired by the National Center for Landscape Fire Analysis (NCLFA) over the LEF located approximately 48 km northeast of Missoula, Montana in the Blackfoot River drainage (N46°53′30″, W−113°26′3″) (Fig. 1). LiDAR data acquisition parameters used for LEF (Table 1) provided an average return density of about 1 return per 2.29 m^2 on the ground with a vertical and horizontal accuracy of 0.15 m and 0.25 m, respectively (Suratno et al., 2009).

Researchers at the NCLFA separated the raw three-dimensional LiDAR points into vegetation (aboveground) and bare earth points using a triangulated irregular network densification method available in the TerraScan software suite (Terrasolid, 2004). Ground points were used to create a digital elevation model (DEM) using inverse distance weighted interpolation at 1 m resolution. The DEM and aboveground points were used to calculate the canopy height model (CHM) using the spot elevation method (Daniels, 2001). This approach computed the canopy height (elevation above ground level) at each point by subtracting the DEM height from the CHM (Suratno et al., 2009).

NCLFA researchers delineated individual trees using a stem identification algorithm based on a combination of variable window local maxima filtering (Popescu and Wynne, 2004) and neighborhood canopy height variance and return density (Rowell et al., 2006). This approach anticipated crown width (CW) as a function of canopy height and stand structure. For a given point in the CHM, the approach searched for higher points within a radius of one half the expected crown width (CW). If no such points were found, the given point in the CHM was assumed to be a tree top. This process was conducted for every point in the CHM to produce a stem map (Suratno et al., 2009). For trees species at LEF, CW was expected to be 33% of the tree height for trees in stands with canopy cover less than 35%, 16% of tree height for trees in stands with moderately closed canopy cover ranging between 35% and 65%, and 11% of tree height for trees in stands with closed canopy cover greater than 65% (Rowell, 2010, Personal communication). Once a tree's location and CW are estimated, a square search window of $2 \times$ CW m centered at the tree location was used to estimate the tree's crown base height (CBH). The tree's CBH was then estimated as the mean height of all CHM points inside the search window divided by the standard deviation of the CHM point heights (Rowell, 2010, personal communication). Individual tree diameter at breast height (DBH) were estimated using the following log-linear model ($n = 1555$, $R^2 = 0.76$, error = 7.6%) (Rowell et al., 2009).

$$\ln \mathrm{DBH} = 1.732 + (0.041 \times \mathrm{HT}) + (0.798 \times \mathrm{RH}) - (0.007 \times \mathrm{SD}) \quad (1)$$

where HT is the height of the tree (m), RH is the relative height calculated as the tree height divided by the mean height of dominant and co-dominant trees in a 20 m × 20 m neighborhood, and SD is stem density of dominant and co-dominant stems in the neighborhood. Tree volumes were estimated using an equation from the Northern Idaho/Inland Empire of the Forest Vegetation Simulation (Keyser, 2008).

$$\mathrm{vol} = \lfloor \{0.00171 \times (d/2.54)^2 \times \mathrm{HT}\} + \{0.00171 \times (d/2.54) \times \mathrm{HT}\} \rfloor \times 0.02831 \quad (2)$$

where vol is the tree volume (m^3), and d is the tree DBH (cm).

2.2. Individual tree fuel connectivity

To quantify fuel connections among individual trees in a stand, we used logistic regression models developed to predict tree-level crown fire initiation and propagation (Contreras et al., 2012). These regression models predict tree-level fuel connectivity under severe weather conditions defined by the 90th percentile of historical observation data from the Seeley Lake (N47°10′58″, W−113°26′50″) weather station located approximately 30 km north of LEF. Weather and fuel moisture parameters used in the development of the model were representative of late summer in the Northern Rocky Mountains and surface fuels were described by parameters similar

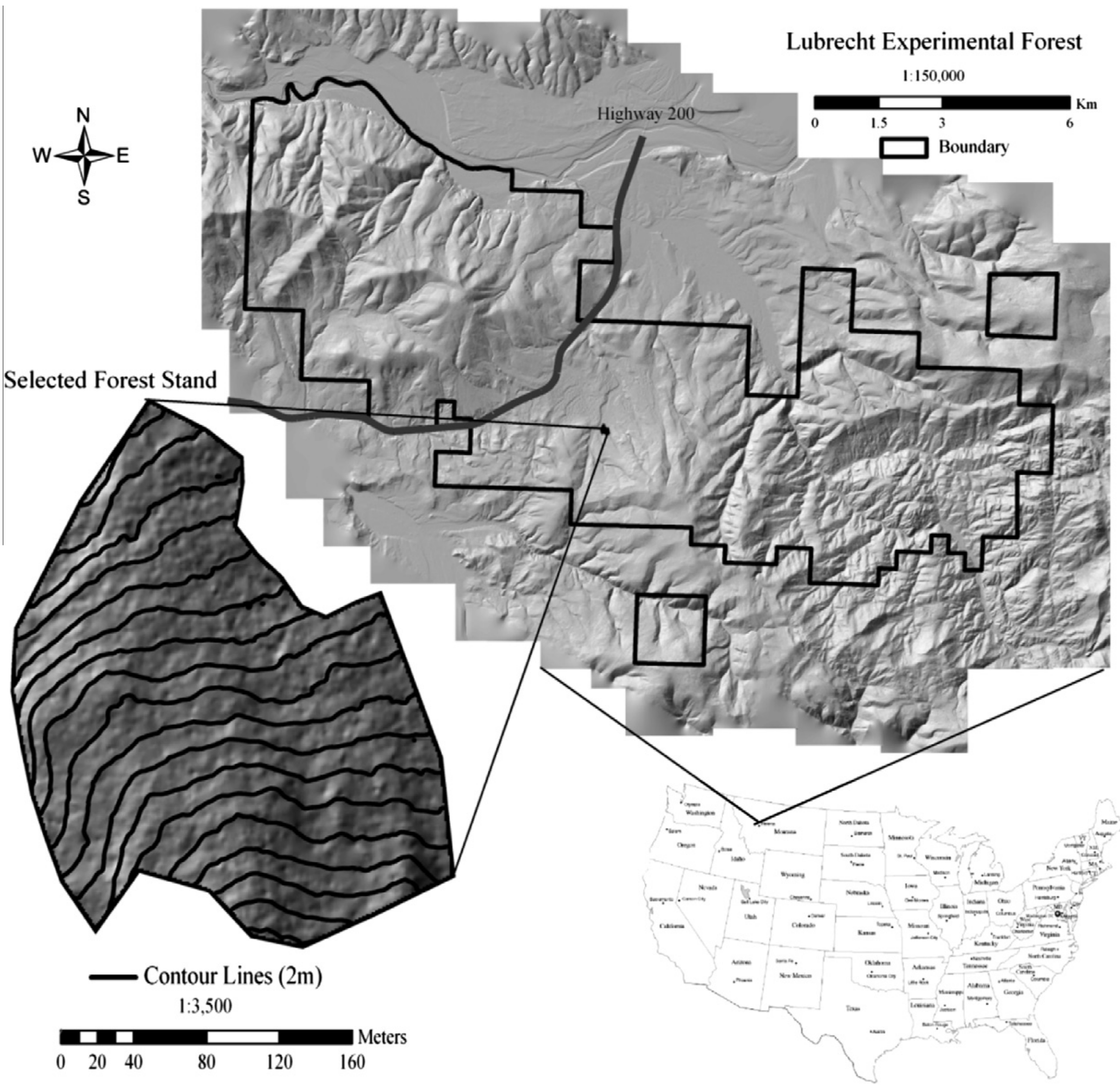

Fig. 1. University of Montana's Lubrecht Experimental Forest located in western Montana (Taken from Contreras et al., 2012.)

Table 1
LiDAR data acquisition parameters used for LEF.[a]

Date of acquisition	June 2005
Elevation	1100–1900 m
LiDAR system	Leica geosystems ALS50
Average flight height above surface	1900 m
Average flight speed	70.76 ms^{-1}
Number of strips	54
Scan frequency	25.5
Laser pulse frequency	36,200 Hz
Scan angle	±35°
Sidelap	50%
Average swath width	1150 m
Average return density	0.44 m^2
Average footprint	1 m^2

[a] Taken from Suratno et al. (2009).

to those representing fuel model 10 (Anderson, 1982). Please refer to Contreras et al. (2012) for more details related to the development of the regression models as well as weather and surface fire inputs.

Crown fire initiation and propagation are predicted by the following logistic regression models:

$$P_{CFI} = \frac{e^{g(x)}}{1+e^{g(x)}}, \quad g(x) = 10.93897 + (0.24285 \times HT) - (2.84814 \times CBH) \tag{3}$$

$$P_{CFP} = \frac{e^{g(x)}}{1+e^{g(x)}}, \quad g(x) = -6.9064 + (0.3194 \times HT) - (3.2356 \times SP) + (69.4118 \times CI_1) \tag{4}$$

where P_{CFI} is the probability that crown fire initiation will occur at a given tree location, P_{CFP} is the probability that fire will propagate crown-to-crown from an ignited source tree representing the flaming front to a target tree ahead of the flaming front. SP is tree spacing measured as the distance (m) between the horizontal crown projections (edge to edge) of the source and target tree. CI_1 is a modified distance-dependent competition index (Rouvinen and Kuuluvainen, 1997) used as a proxy for size and proximity of the flaming front approaching the target tree. It is calculated as the sum of the horizontal angles originating from the center of the target tree and spanning the DBH of each tree forming the flaming front (Eq. (5)). The model uses a flaming front area of 1.5 m × 10 m centered on the source tree to search for additional trees forming the flaming front (Fig. 2).

$$\mathrm{CI}_1 = \sum_{i=1}^{n} \arctan(d_i/\mathrm{dist}_i) \tag{5}$$

where n is the number of trees forming the approaching flaming front, d_i is the DBH (cm) of the ith tree forming the flaming front, and dist_i is the horizontal distance (m) from the center of the ith source tree to the center of the target.

To use these regression models deterministically, we applied the same threshold probability of 0.5 used by Contreras et al. (2012) because it adequately captured the binary nature of tree-level fuel connections. In their study, simulation results showed that trees either ignited burning crown fuels completely or did not ignite. Similarly, when fire propagated from a source tree to a target tree, the crown fuels of the target tree burned completely. Therefore, when $P_{CFI} > 0.5$, crown fire initiation is expected to occur and the tree's crown fuels are considered vertically connected with surface fuels. Similarly, fire is expected to propagate from an ignited source tree to the target tree when $P_{CFP} > 0.5$, considering both tree crown fuels horizontally connected.

2.3. Individual tree distance-dependent growth model

We used an individual tree distance-dependent growth model developed to predict average annual basal area increment (BAI) for three common tree species in LEF; Douglas-fir (*Pseudotsuga menziesii* [Mirbel] Franco var. *glauca* [Beissn.] Franco), ponderosa pine (*Pinus ponderosa* Dougl. ex Laws.), and western larch (*Larix occidentalis* Nutt), (Contreras et al., 2011). The model is based on neighboring tree data collected for 285 cored trees within an 11-m plot radius. Tree cores were measured and average BAI (cm^2/year) was computed for a 10 year period from 1998 to 2007.

The individual tree growth model has the expression:

$$\mathrm{BAI} = \exp[0.0624 + 0.773\ln(\mathrm{DBH}) - 0.343\mathrm{CI}_2] \tag{6}$$

where CI_2 is a distance-dependent competition index calculated similar to CI_1. It is calculated as the sum of the horizontal angles originating from the subject tree center and spanning the DBH of each neighbor tree inside the 11-m plot radius (Eq. (7)) (Rouvinen and Kuuluvainen, 1997).

$$\mathrm{CI}_2 = \sum_{j=1}^{ng} (d_j/d) \times \arctan(d_j/\mathrm{dist}_j) \tag{7}$$

where d_j is the DBH (cm) of the jth neighbor tree, dist_j is the horizontal distance (m) from the subject tree center to jth neighbor tree center, and ng is the number of neighbor trees inside the 11-m radius plot.

After the average annual BAI was estimated for a given tree (Eq. (6)), expected future DBH was calculated. Future HT was then obtained using a logistic height–diameter equation from the Northern Idaho/Inland Empire of the Forest Vegetation Simulation (Keyser, 2008).

$$\mathrm{HT} = \left[4.5 \times e^{\{4.81519 - 7.29306/((d/2.54)+1.0)\}}\right] \times 0.3048 \tag{8}$$

Expected future CW was estimated as 16% of tree height assuming a future stand structure would have moderately closed canopy. Future CBH was estimated assuming it increases proportionally to HT. We made these assumptions because of the lack of future vegetation data necessary for projecting CHM over 20 years (Rowell, 2010, Personal communication).

2.4. Individual tree timber harvesting cost

We used a computerized model developed to estimate skidding costs of individual trees for ground-based harvesting operations (Contreras and Chung, 2011). The model considers size and spatial distribution of individual cut-trees and detailed terrain information obtained from a LiDAR-derived stem map and DEM, respectively. First, the model uses a log-bunching algorithm to identify the location and volume of log-piles. A cable skidder operation, which collects nearby cut-trees within a maximum winching radius (MWR) through a cable winch, is simulated to complete a full load close to a target loading capacity (TLC) and skid the load to an extraction point (landing or road side). The log-bunching algorithm begins with sorting all cut-trees based on their slope distance from the extraction point. The algorithm selects the closest cut-tree as the first log-pile location, and all cut-trees within the MWR from the log-pile with a combined volume lower than the TLC are assigned to the first log-pile. Then, the algorithm selects the next closest non-assigned cut-tree as the second log-pile location, and assigns nearby cut-trees within the MWR to the second log-pile. The process continues until all cut-trees have been assigned to a log-pile. The model then determines least-cost routes connecting each log-pile to the extraction point by developing a skid-trail network formed by vertices and edges. Each vertex, which represents

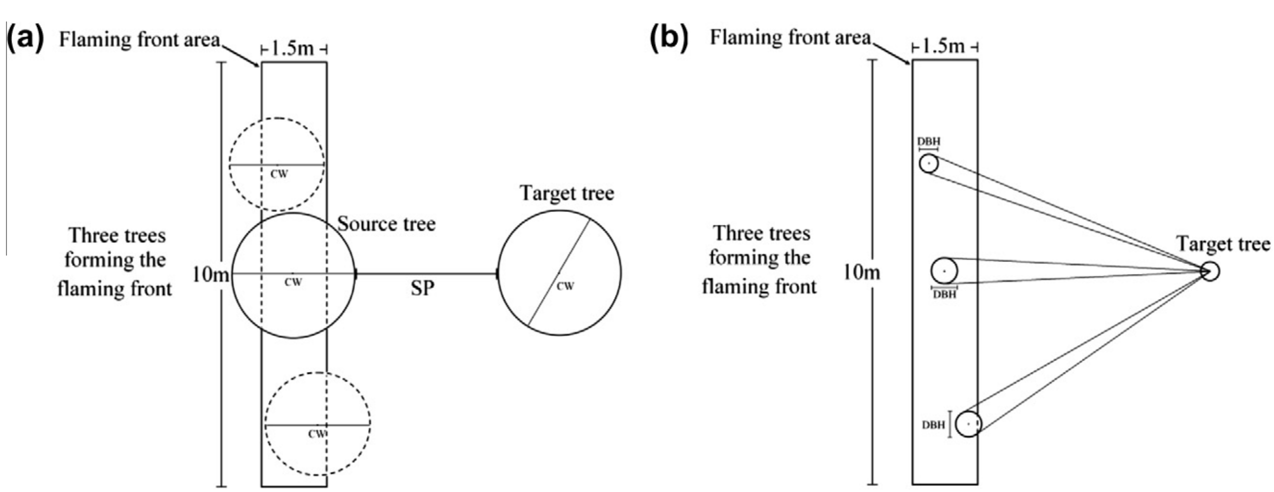

Fig. 2. Schematic of the flaming front area used to search additional source trees (dashed lines) showing spacing between a source tree and a target tree (solid lines) (a) and the calculation of CI_1 (b) to estimate fuel connectivity.

the center of a DEM cell evenly spaced at a 5-m interval, is connected to its eight adjacent vertices. Edges represent the connection (skid-trail links) between a vertex and its adjacent neighboring vertices. The model then creates feasible skid-trail links over areas with gentle to moderate slope (i.e., lower than 35%). To avoid damage to remaining trees, no skid-trail links are allowed within 1.5 m of each leave-tree.

After the skid-trail network has been created, the model determines the skidding cycle time associated with each link based on its distance and slope, using the skidding cycle time models presented in (Contreras and Chung, 2007).

$$CT_{ds} = 3.9537 + (0.0215 \times D) \quad (9)$$

$$CT_{us} = 3.9537 + (0.0258 \times D) \quad (10)$$

where CT_{ds} is the cycle time (min) for downhill skidding, CT_{us} is the cycle time (min) for uphill skidding, and D is the slope distance of the skid-trail link (m).

Skidding cycle time is used as an edge attribute to formulate a network problem. The model uses the Dijkstra's shortest path algorithm (Dijkstra, 1959) to find least cycle time routes connecting each log-pile to the extraction point. The skidding cost for a given ith log-pile (PSC_i) is estimated using the following equation:

$$PSC_i = \left(\frac{CT_i}{60}\right) \times RR \quad (11)$$

where CT_i is the least skidding cycle time (min) for a round trip between the extraction point and the ith log-pile location, and RR is the rental rate of the skidder ($/h). Skidding cost of individual trees is estimated by prorating the log-pile's skidding cost based on the volume ratio of the individual tree to the entire log-pile (Eq. (12)). Thus, bigger cut-trees entail a larger skidding cost than smaller cut-trees in the same pile.

$$TSC_j = \left(\frac{vol_j \times PSC_i}{Pvol_i}\right) \quad (12)$$

where TSC_j is the skidding cost ($) of the jth individual cut-tree, vol_j is the volume (m^3) of the jth cut-tree, PSC_i is the skidding cost ($) of the ith log-pile containing cut-tree j, and $Pvol_i$ is the volume (m^3) of the ith log-pile.

2.5. Individual tree removal optimization

To ensure the effectiveness and efficiency of thinning treatment on reducing crown fire potential over time, we considered a period of 20 years and applied the tree-level growth model to estimate future tree sizes. We used the crown fire initiation and propagation models to predict current fuel connections among existing tree and future fuel connections among remaining trees after treatment. The selection of individual cut-trees is optimized based on current fuel connections among all trees, expected future fuel connections after removing the cut-trees and growing the remaining leave-trees for 20 years, and the cost associated with skidding the selected cut-trees.

The tree removal optimization problem is formulated as follows:

$$\text{Minimize} \quad Z = \left[\sum_{i=1}^{NT}(TSC_i \times \{1 - I_i\})\right] + \left[\sum_{i=1}^{NT}[(CHFC_i + CVFC_i + FHFC_i + FVFC_i) \times I_i]\right] \quad (13)$$

$$\text{subject to} \quad \sum_{i=1}^{NT}\{1 - I_i\} = TCT \quad (14)$$

where I_i is a binary variable indicating whether the ith tree remains ($I_i = 1$, leave-tree) or is removed from the stand ($I_i = 0$, cut-tree), $CHFC_i$, and $CVFC_i$ are coefficients representing the number of current horizontal and vertical fuel connections associated with the ith tree, $FHFC_i$ and $FVFC_i$ are coefficients representing the number of future horizontal and vertical fuel connections associated with the ith tree, TSC_i is the skidding cost ($) associated with skidding the ith tree, and NT is the total number of trees. The objective function (Eq. (13)) represents an index number set to minimize the skidding cost (first term) and number of fuel connections (second term). Due to the lack of data relating expected economic losses and tree-level fuel connectivity in the application presented in this study, skidding cost and fuel connections have the same weight in the objective function giving the same importance to both factors. More research is needed to determine the relative importance of each factor under different management scenarios and evaluate the effects of these weights of the optimal selection of trees to remove. Eq. (14) is a constraint ensuring that the target thinning intensity in terms of the number of trees is met, where TCT is the target number of cut-trees.

We used a network to model fuel connectivity and solve the tree removal optimization problem. A fuel connectivity network consists of a set of vertices v, which represent tree locations, and a set of edges E representing fuel connections between pairs of adjacent trees. Our approach starts with applying the crown fire initiation and propagation regression models to estimate current fuel connections among trees and form the fuel connectivity network. Clusters of connected trees are identified in the fuel connectivity network and characterized in terms of number of trees forming each cluster (ρ). Fig. 3 shows an example of a fuel connectivity network formed by 43 trees, resulting in nine clusters of connected trees with sizes ranging from 1 to 16. Each cluster represents the extent fire would propagate and the number of trees that would burn after fire reaches crown fuels through vertical fuel connections.

For the purpose of reducing crown fire potential by breaking fuel connectivity throughout a forest stand, we determined the minimal combination of cut-trees required to remove all horizontal fuel connections within each cluster of connected trees. This was achieved by using an algorithm to identify a minimal vertex cover (MVC) in a graph G. A vertex cover C of G is a set of vertices such that for each edge $\{u, v\}$ in G, at least one of its vertices u or v

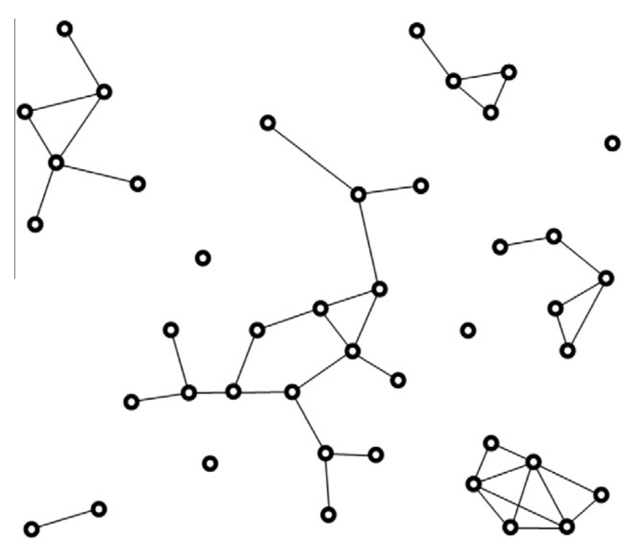

Fig. 3. Example of a fuel connectivity network formed by 43 vertices and nine clusters of connected trees.

is in C. Given a vertex cover C of G and a vertex v in G, v is removable if the set $C - \{v\}$ is still a vertex cover of G. A MVC is then a vertex cover with no removable vertices. In our context, a MVC represents the minimal combination of cut-trees required to remove all fuel connections.

2.5.1. MVC algorithm

Given a graph G, all vertices are labeled consecutively from $1, 2, \ldots, p$. Starting with the first vertex ($i = 1$), the vertex cover is initialized as $C_i = v - \{i\}$. If C_i has no more removable vertices, we stop and store the size $\varphi(C_i)$ of the vertex cover C_i. Otherwise for each removable vertex v of C_i, we find the number $\psi(C_i - \{v\})$ of additional removable vertices of the vertex cover $C_i - \{v\}$. We denote the $v_{\max}$ as the removable vertex such that $\psi(C_i - \{v\})$ is maximum, and then update the vertex cover as $C_i = C_i - \{v_{\max}\}$. When multiple vertices with the same $\psi(C_i - \{v\})$ value exist, we arbitrarily select the first one. Thereafter, vertex $v_{\max}$ is selected and removed from C_i ($C_i = C_i - \{v_{\max}\}$). The process of removing $v_{\max}$ vertices and updating the vertex cover C_i is repeated until no more removable vertices exit. When the process is finished, the MVC initialized with C_i is obtained. Now we move to the next vertex ($i = i + 1$) and initialize the vertex cover $C_i = v - \{i\}$ and obtain the associated MVC. We stop when a MVC is obtained for all vertices in G. All resulting MVC are stored and ordered by ascending sizes $\varphi(C_i)$. The MVC with minimum size is selected as the final MVC of G. Table 2 shows the steps required to obtain the MVC initialized with the first vertex in a graph with nine vertices.

The total number of cut-trees required to remove all fuel connections (RCT) is then determined by summing up the size of the final MVC for each cluster

$$\mathrm{RCT} = \sum_{i=1}^{\omega} \varphi_i \tag{15}$$

where ω is total number of clusters in the fuel connectivity network.

Three cases arise when evaluating the thinning intensity constraint (Eq. (14)). In case I, the target number of cut-trees is equal to the number of trees required to remove all fuel connections (RCT = TCT). There are a large number of combinations of cut-trees that remove all fuel connections because most clusters have multiple final MVC of same size. We select final MVC based on their proximity to the extraction point, measured as the average slope distance (AD_MVC) from all vertices (cut-tree locations) forming the MVC to the extraction point. The jth final MVC of the kth cluster in the fuel connectivity network is then selected based on a random number and a selection probability calculated by

$$\mathrm{SP\_MVC}_{jk} = \frac{\mathrm{AD\_MVC}_j^{-1}}{\sum_{i=1}^{cn} \mathrm{AD\_MVC}_i^{-1}} \tag{16}$$

where $\mathrm{SP\_MVC}_{jk}$ is the selection probability that the jth final MVC of the kth cluster is selected, and cn is the number of final MVC of the same size associated to the kth cluster in the fuel connectivity network.

Case II represents the case where the target number of cut-trees is smaller than the number of trees required to remove all fuel connections (TCT < RCT). In this case, additional leave-trees (ALT) need to remain to meet the thinning intensity constrain. The number of additional leave-trees is calculated (ALT = RCT − TCT), and leave-trees are selected based on both their proximity to the extraction point and the number of remaining fuel connections. After selecting a final MVC for each cluster in the fuel connectivity network (Eq. (16)), additional leave-trees are selected based on the selection probability calculated as follows:

$$\mathrm{SP\_LT}_j = \frac{(1 - \mathrm{SAD\_T}_j) + \mathrm{SFC\_T}_j}{\sum_{i=1}^{\mathrm{ALT}} (1 - \mathrm{SAD\_T}_i) + \mathrm{SFC\_T}_i} \quad \forall j \in P \tag{17}$$

where $\mathrm{SP\_LT}_j$ is the selection probability that the jth tree is selected to remain, $\mathrm{SAD\_T}_j$ is the standardized slope distance from the jth tree to the extraction point, $\mathrm{SFC\_T}_j$ is the standardized number of fuel connections between the jth tree and other already selected leave-trees, and P is the set of trees forming the selected final MVC for all clusters. Standardized values were used to reduce slope distance and the number of fuel connections to the same scale and give equal weight to both factors when calculating the tree selection probability.

For case III, the target number of cut-trees is larger than the number of trees required to remove all fuel connections (RCT < TCT). Here, additional cut-trees need to be selected for removal. The number of additional cut-trees is calculated (ACT = TCT − RCT), and cut-trees are selected based on their proximity to the extraction point

$$\mathrm{SP\_CT}_j = \frac{\mathrm{AD\_T}_j^{-1}}{\sum_{i=1}^{\mathrm{ACT}} \mathrm{AD\_T}_i^{-1}} \quad \forall j \in S \tag{18}$$

where $\mathrm{SP\_CT}_j$ is the selection probability that the jth tree is selected to be removed, $\mathrm{AD\_T}_j$ is the slope distance from the jth tree to the extraction point, and S is the set of trees not belonging to the selected MVC for any cluster in the fuel connectivity network (originally selected leave-trees).

As mentioned above, our computerized approach starts with applying the crown fire initiation and propagation regression models to estimate current tree-level fuel connections among all trees. Then, the number of fuel connections for each tree and the size of clusters of connected trees are calculated. The approach builds a solution by (i) randomly selecting a MVC for each cluster as well as additional cut- or leave-trees (depending on the constrain case) based on the number of fuel connections and proximity to the extraction point (Eqs. (16)–(18)), (ii) estimating the skidding cost of selected cut-tree the number of fuel connections among selected leave-trees, (iii) applying the individual tree growth model to estimate future tree sizes, and (iv) applying the crown fire initiation and propagation models to estimate future tree-level fuel connections among selected leave-trees. The solution is then evaluated and the objective function value (Eq. (13)) is stored. For next solution, a different random combination of cut-and leave-trees is generated, and the objective function is evaluated and compared with the previous solution. If the current solution is better than the previous one (lower total skidding cost and lower number of current and future fuel connections), it is stored and saved as the best solution found. Otherwise, the current solution is ignored and another solution is generated. This iterative process of generating and evaluating alternative solutions (combinations of cut- and leave-trees) continues until a stopping criterion is met. We used a maximum number of solutions, $S_{\max}$, to stop the process in a reasonable amount of time. When the process stops the best solution found is reported. For the model application presented in this study, we set $S_{\max}$ at 15,000 solutions.

2.6. Model application – a case study

The study area for this investigation is a forest stand in the LEF (Fig. 4). The stand is 4.6 ha in size with elevations ranging from 1270 to 1310 m, on a north-facing aspect, and an average slope of 13.5% (0.0–36.3% slope range). Douglas-fir is the dominant species with a small amount of ponderosa pine trees. The stand has established under- and middle-story vegetation creating continuous canopy fuels from the ground to the top of the canopy, resulting from logging in the mid-1940s and thinning in the mid-1970s.

Table 2
Steps required to obtain the MVC initialized with vertex number one.

	Removable vertex v of C_1	Additional removable vertices of $C_1 - \{v\}$	$\psi(C_1 - \{v\})$
Step 1: We initialize the vertex cover as $C_1 = v - \{1\} = \{2, 3, 4, 5, 6, 7, 8, 9\}$, size $\varphi(C_1) = 8$			
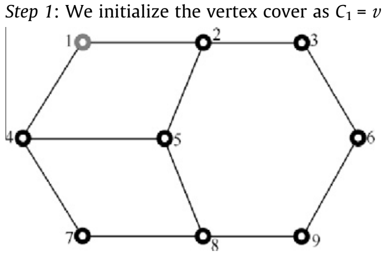	3	5, 7, 8, 9	4
	5	3, 6, 7, 9	4
	6	5, 7, 8	3
	7	3, 5, 6, 9	4
	8	3, 6	2
	9	3, 5, 7	3
Maximum $\psi(C_1 - \{v\}) = 4$ for $v = 3, 5, 7$. We arbitrarily remove vertex 3 from C_1			
Step 2: Vertex cover $C_1 = \{2, 4, 5, 6, 7, 8, 9\}$, size $\varphi(C_1) = 7$			
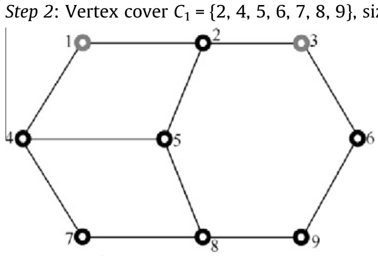	5	7, 9	2
	7	5, 9	2
	8	None	0
	9	5, 7	2
Maximum $\psi(C_1 - \{v\}) = 2$ for $v = 5, 7, 9$. We arbitrarily remove vertex 5 from C_1			
Step 3: Vertex cover $C_1 = \{2, 4, 6, 7, 8, 9\}$, size $\varphi(C_1) = 6$			
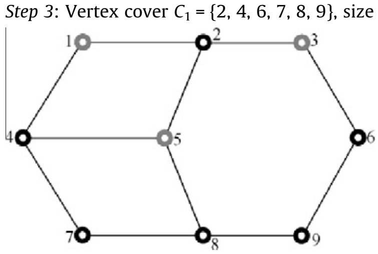	7	9	1
	9	7	1
Maximum $\psi(C_1 - \{v\}) = 1$ for $v = 7, 9$. We arbitrarily remove vertex 7 from C_1			
Step 4: Vertex cover $C_1 = \{2, 4, 6, 8, 9\}$, size $\varphi(C_1) = 5$			
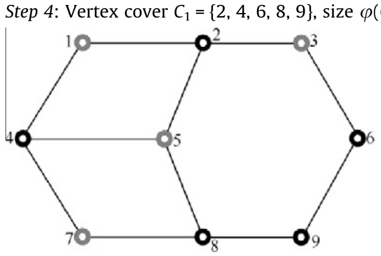	9	None	0
Maximum $\psi(C_1 - \{v\}) = 0$ for $v = 9$. We remove vertex 9 from C_1			
Step 5: Vertex cover $C_1 = \{2, 4, 6, 8\}$, size $\varphi(C_1) = 4$			
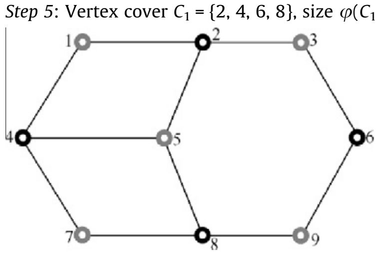	None	–	–
Step 6: We stop and obtain a MVC, C_1 of size $\varphi(C_1) = 4$			

The LiDAR stem detection algorithm identified over 11,000 trees in the stand, most of which are small, suppressed trees. For the purpose of reducing crown fire potential, we first considered an initial thinning prescription that cuts, piles, and burns small trees with DBH less than 12.5 cm (5 in.). Fig. 4b presents the LIDAR-derived stem map showing the remaining 2645 individual tress in the study area after the initial thinning prescription was applied. Cut-tree selection was then optimized for the remaining trees to meet a target tree density of 300 leave-trees per ha or TCT = 1265 trees.

3. Results and discussion

Based on the current LiDAR-derived tree locations and attributes, fuel connectivity models predicted tree-level vertical fuel connections with surface fuels and horizontal fuel connections between adjacent trees (Table 3). Vertical fuel connections, representing the ignition of crown fuels, were predicted at 536 tree locations, representing over 20% of tree in the stands. Crown fire propagation models predicted over 27,500 horizontal fuel connec-

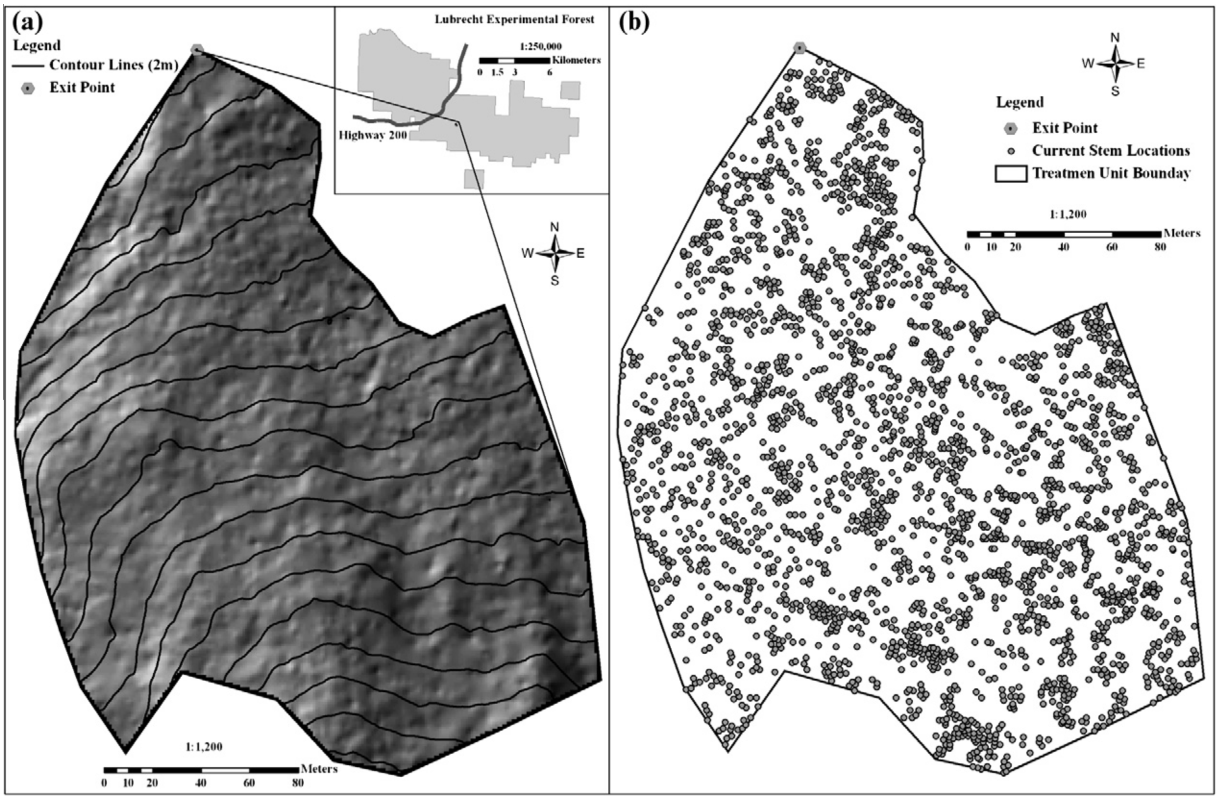

Fig. 4. LiDAR-derived digital elevation model (a) and stem map (b) for the 4.6-ha study area in LEF. Figure b was taken from Contreras et al. (2012).

tions between adjacent pairs of trees, mainly due to the relatively larger number of trees and dense stand structure. These horizontal fuel connections resulted in a fuel connectivity network formed by 38 clusters of connected trees (Table 3). In average, clusters are formed by about 70 connected trees, and crown fuels of each tree are connected to an average of about 10 adjacent trees. Most clusters are formed by less than 15 connected trees. However, the single largest cluster connects over 92% of trees in the stand (Fig. 5). These results indicate that, after reaching crown fuels through vertical fuel connections, fire can propagate throughout the stand burning most trees in the study area. The large number of fuel connections, average connections per tree, and average connections per cluster also indicate a relatively high crown fire potential under the current stand structure.

The MVC algorithm was applied to the cluster forming the fuel connectivity network to identify all possible final MVC associated with each cluster. Adding the size of the final MVC for each cluster resulted in a total of 1996 cut-trees were required to remove all fuel connections (RCT) in the study area. This would results in only 649 leave-trees corresponding to a thinning intensity of over 75% of total number of trees. Consequently, as RCT is larger than the TCT (1996 vs. 1265 – constraint case II), 731 additional leave-trees were required to be selected to meet the thinning intensity constraint of 300 trees per ha.

For each solution, the computerized approach randomly selected MVC for each cluster (Eq. (16)) and additional leave-trees (Eq. (17)) to generate an alternative combination of cut- and leave-trees. Objective function value was evaluated by quantifying tree-level fuel connections among selected leave-trees, skidding costs of selected cut-trees, and future tree-level fuel connections among selected leave-trees after applying the growth models for a period of 20 years. The best solution found by the computerized approach was found after generating about 12,000 alternative combinations of cut- and leave-trees. Fig. 6 shows the improvement of the objective function values over the random search optimization process. The best solution found has an objective function value of 13,706; consisting of 4366 remaining fuel connections (315 vertical and 4051 horizontal), 5837 future fuel connections (189 and 5648 vertical and horizontal, respectively) among the selected leave-trees, and a skidding cost of 3503 associated with the selected cut-trees. As mentioned above, the objective function value represents an index number combining fuel connections and skidding cost, with equal weight to both factors.

Fuel connectivity throughout the study area was largely reduced by removing about 48% of the total number of trees in the study area (1265 cut-trees). The best solution found by computerized approach identified a combination of cut-trees that reduced fuel connectivity by almost 85%, from over 28,000 fuel connections under current stand conditions to about 4365 fuel connections after treatment (Fig. 7). Also, the number of trees expected to ignite decreased by about 41% from 536 to 315 trees. The number of clusters of connected trees increased from 38 to 173 indicating a large increase in fuel discontinuity. The average number of tree forming a cluster was lowered from almost 70, under current conditions, to about 8 after treatment, and the average fuel connections per tree decreased from over 10 to about 4 (see Table 3). Similarly to the current conditions before treatment, most clusters are formed by less than 15 connected trees. However, 5% of clusters now connect about 72% of leave-trees after treatment and the largest cluster connects only about 59% of leave-trees.

The individual distance-dependent tree growth model was applied to the selected leave-trees based on tree locations and sizes to estimate tree growth under the new stand conditions after the thinning treatment. Average periodic increment in DBH of leave-trees was 5.08 cm for a 20-year period (Table 4). Based on the estimated future DBHs and the height–diameter relationship (Eq. (8)),

Table 3
Tree-level fuel connectivity results from the logistic regression models for trees under the current stand condition and the projected future condition after a 20-year growing period.

Stand condition	Crown fire initiation		Crown fire propagation				
	Number of trees ignited	Percentage of trees ignited	Horizontal fuel connections	Number of connected clusters	Average connections per cluster	Average connection per tree	Average trees per cluster
Current	536	20.26	27,755	38	730.39	10.49	69.60
After thinning	315	22.68	4051	173	23.41	2.94	7.98
Future	189	17.68	5648	56	100.86	4.09	24.64

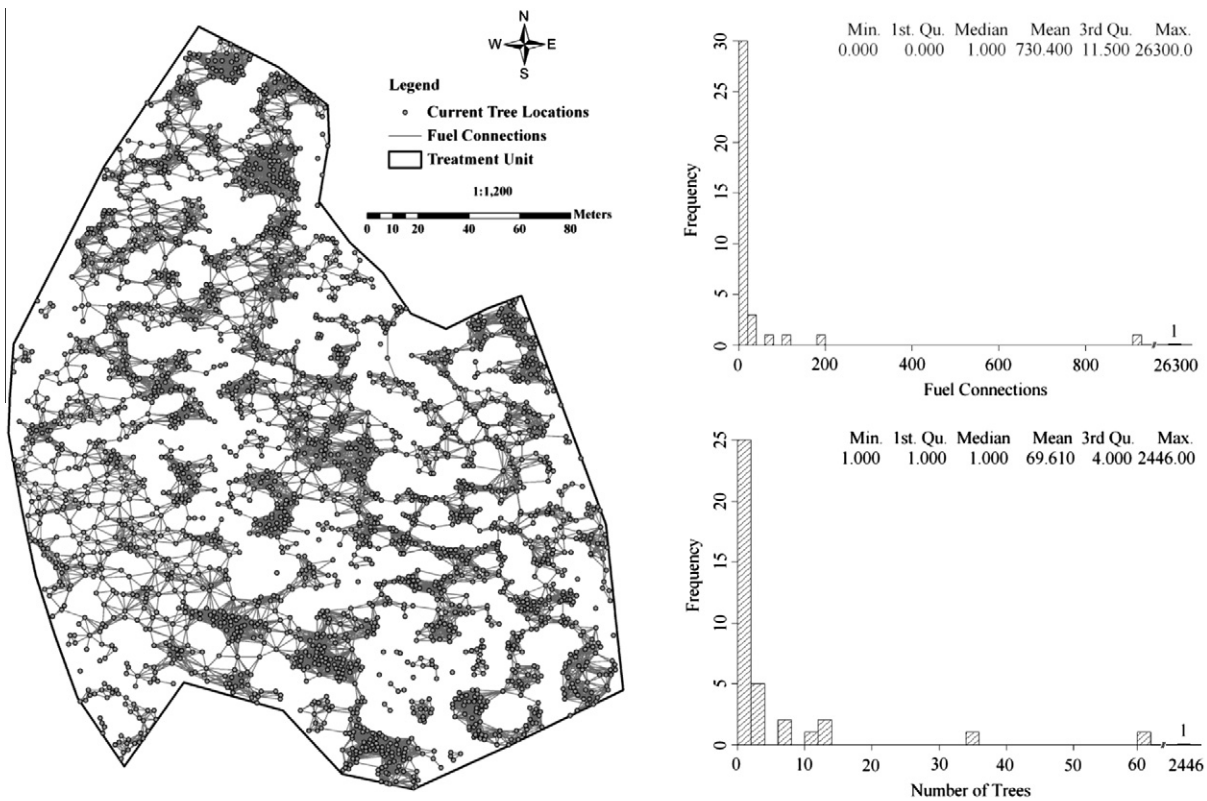

Fig. 5. Location, size, and summary statistics of clusters formed by predicted tree-level fuel connections under the current conditions in the study area.

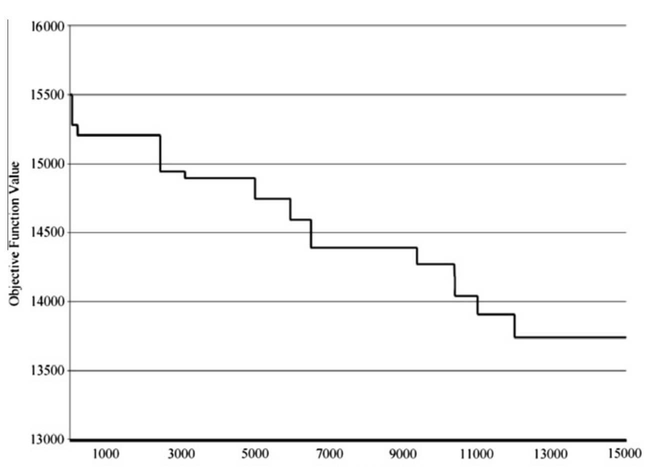

Fig. 6. Change in the objective function value over the 15,000-solution random search optimization process (the best solution was found at solution 12,023).

future tree HT were estimated to increase by an average of 34% (e.g., 5.27 m). As CBH was assumed to increase in the same proportion as tree HT, the average future CBH was also estimated to increase by about 34%. Lastly, CW was expected to increase by an average of 0.47 m (Table 4).

As expected, the total number of tree-level fuel connections among the selected leave-trees was predicted to increase over the 20-year period due to tree growth. The number of vertical fuel connections was reduced from 315 after treatment to 189 under future stand conditions (see Table 3). This result is due to our assumption of growing CBH over time, but in practice the gap between surface and crown fuels might even decrease due to regeneration, which was not considered in our analysis because of the lack of more comprehensive forest dynamic models. The number of horizontal fuel connections rose by about 39%, from 4015 under stand conditions after treatment to 5648 under future stand conditions (see Table 3), as a result of tree growth and reduced spacing between adjacent pairs of leave-trees. The reduction in the number of clusters of connected trees (173 vs. 56), the increase in the average cluster size (from about 8 to almost 25), and average fuel connections per tree (from 2.94 to 4.09) are also indicators of an increased fuel connectivity under future stand conditions (see Table 3). Fig. 8 shows the location and sizes of clusters formed by future horizontal fuel connections among leave-trees. Although future fuel connectivity increased throughout the study area com-

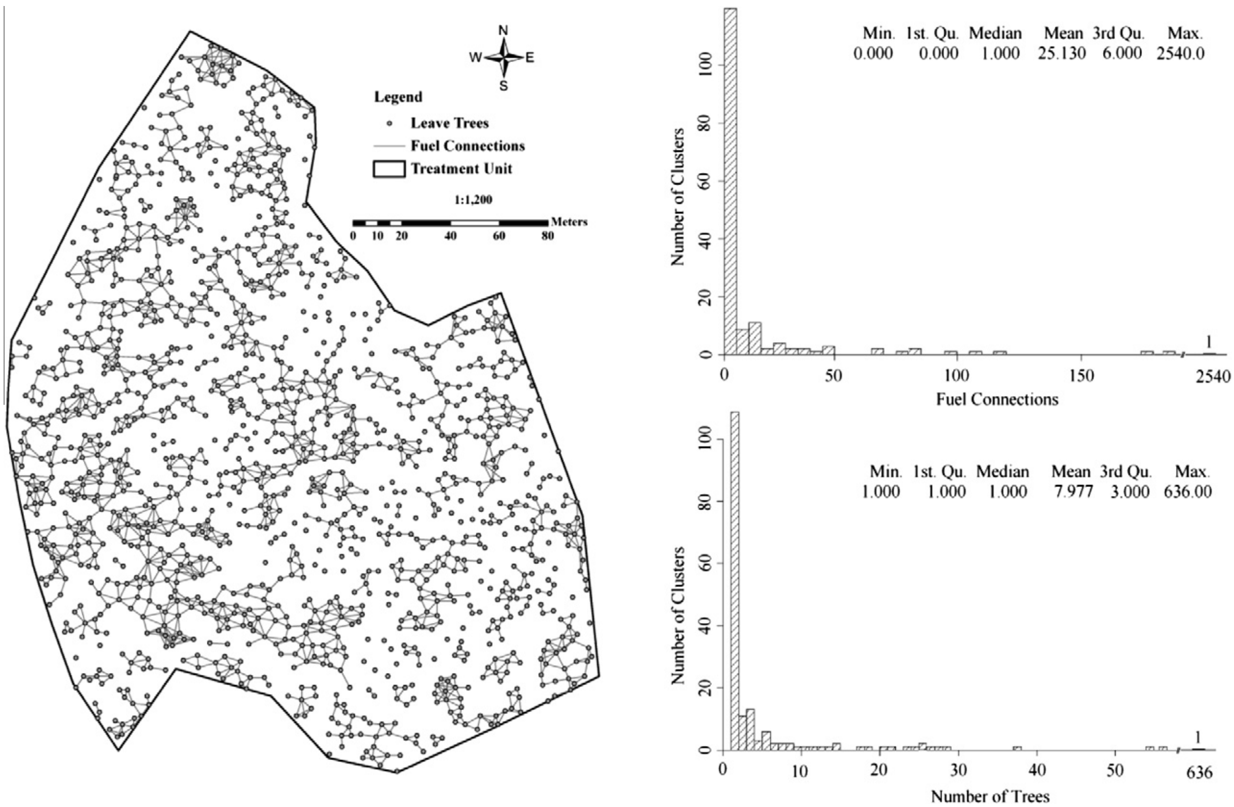

Fig. 7. Leave-tree locations and summary statistics of clusters formed by remaining fuel connections found by the best solution.

Table 4
Current and future tree attributes predicted using the individual tree growth model over a 20 year period.

Time	Tree attribute	Range of values						Periodic increment over 20 years
		Min.	1st Qu.	Median	Mean	3rd Qu.	Max.	
Current	HT	8.79	12.23	14.96	15.51	17.93	33.05	5.27 m (33.98%)
Future		15.77	18.41	20.31	20.78	22.68	35.79	
Current	DBH	12.70	15.46	19.40	21.56	25.18	60.85	5.08 cm (23.53%)
Future		16.76	20.86	24.48	26.64	30.09	66.00	
Current	CBH	0.00	5.33	6.99	7.06	9.03	15.08	2.48 m (34.18%)
Future		0.11	7.47	10.45	9.54	11.81	19.00	
Current	CW	2.34	3.67	4.49	4.65	5.38	9.91	0.47 m (9.92%)
Future		2.64	4.04	4.94	5.12	5.92	10.90	

pared with the stand conditions right after thinning, crown fire potential remains still relatively low after 20 years. The number of future tree-level fuel connections is about 20%, the average cluster size is one third, and the average connections per tree is about 40% compared with the stand conditions before thinning.

The individual tree skidding cost model identified log-pile locations and the optimal skid-trail network connecting each log-pile to the extraction point that ensures the cost efficiency of the thinning treatment (Fig. 9). Based on the location and sizes of the 1245 cut-trees selected by the computerized approach (Fig. 9a), the log-bunching algorithm identified 275 log-piles (Fig. 9b). A skid-trail network composed of almost 3450 feasible skid-trail links was created over the study area based on; terrain conditions (represented by the LiDAR-derived DEM), and the location of the 275 log-piles and the remaining 1380 leave-trees (Fig. 9c). The Dijkstra's shortest path algorithm identified the optimal skid-trail network that minimizes the skidding cost from each log-pile to the extraction point was developed, which is formed by about 1080 ski-trail links. Fig. 9d shows the optimal skid-trail network with traffic level on each skid-trail link in terms of the number of passes (turns). The resulting average skidding cost per log-pile is about \$12.5 and the average skidding distance from a log-pile to the exit point is about 224 m (Table 5). Fig. 10a shows the range of skidding costs per log-pile. Log-piles located farther away from the exit point have larger skidding costs. Skidding costs of individual cut-trees ranged from \$0.19 to about \$17 with an average of \$2.8 (Table 5). Cut-trees with large skidding costs can be found throughout the study area because cost is a function of both tree size and distance from the extraction point (Fig. 10b).

3.1. Model validation

As mentioned above, the best tree removal selection found by the computerized approach appears to largely reduce crown fire potential as measured by the tree-level fuel connectivity. However, it is difficult to ensure solution quality due to the lack of efficient optimization algorithms (i.e., mixed-integer programming) capable of solving the tree removal problem to optimality within a reasonable amount of computing time. With the purpose of benchmarking solution quality, we compared the best solution

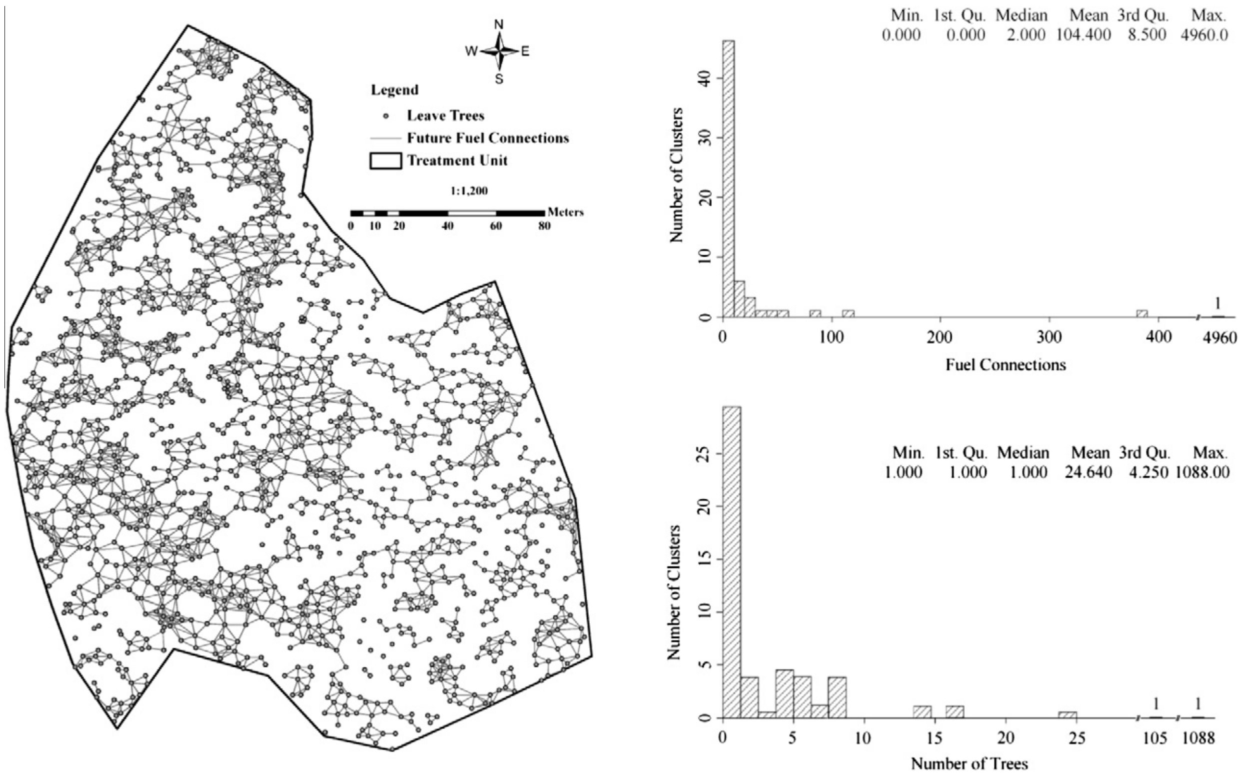

Fig. 8. Leave-tree locations and summary statistics of clusters formed by future fuel connections after a 20-year growth period.

found with two alternative combinations of cut- and leave-trees under the same thinning intensity (1380 leave-trees and 1265 cut-trees). The first alternative combination consists of cut-trees selected manually simulating the marking process carried out by markers on the ground based on spacing between trees and tree sizes. During the manual selection of cut-trees, we visually identified dense groups of trees on the stem map (Fig. 4b). Within these dense groups of trees, the tree with largest DBH was selected as a leave-tree and remove (mark as cut-trees) all smaller trees within a 2.5 m radius. The process of removing trees (selecting cut-trees) continued until the target thinning intensity was met. The second alternative combination selected cut- and leave randomly. In this random combination a given leave-tree was selected by (i) indexing all 2645 trees in the stand, (ii) generating a random number from 1 to 2645, and (iii) selecting the tree indexed with the selected random number as a leave-tree. This combination of random leave-trees was completed when 1380 distinct leave-trees were selected. For each of these two alternative selections of cut- and leave-trees, we evaluated the objective function value by estimating the (i) number of tree-level fuel connections between adjacent pairs of leave-trees after treatment and under future stand conditions and (ii) skidding costs associated with the selected cut-trees. The manual and random cut- and leave-tree selection resulted in objective function values about 5% and 34% higher than the objective function value of the best solution found by the computerized approach, respectively (Table 6).

Skidding costs of the optimal solution (computerized approach) and two alternative solutions (random and manual) are within 5%, but the number of remaining and future fuel tree-level fuel connections varied widely among solutions. The manual solution has a slightly smaller skidding cost and a slightly larger number of remaining fuel connections than the optimal solution. However, the manual solution resulted in more than 450 additional future fuel connections compared with the optimal solution. This indicates that, although a manual selection of cut- and leave-trees could produce similar results to the optimized tree removal, the manual selection might inefficiently evaluate the temporal effects of tree selection for reducing crown fire potential over time. On the other hand, the random tree selection resulted in a much larger number of remaining and future tree-level fuel connections (see Table 6), which shows a large variability in tree-level fuel connectivity among alternative selections of trees. Our approach, besides optimizing the cut- and leave-tree selection, provides a more consistent and objective method to evaluate alternative cut-tree patterns and improves the efficiency of thinning treatments for reducing crown fire potential over time. Lastly, identifying selected individual trees is likely to be more time consuming when implementing the optimal or random tree selection, thus, tree-marking is likely to be more productive when implementing the manual tree selection method. Future comparisons should also consider the practical aspects of tree-marking on the ground and evaluate the cost efficiency of implementing model results.

Our computerized approach to optimize the selection of tree removal can efficiently break fuel connectivity throughout a forest stand to reduce crown fire potential. However, the results of the computerized approach depend heavily on the accuracy of input data such as tree locations, as well as current and estimated future tree dimensions. There are several ways to acquire tree locations varying from traditional field measurements and GPS devises to advanced remote sensing and GIS technologies such as high-resolution aerial photos (Hirschmugl et al., 2007), multispectral imaging (Popescu and Wynne, 2004), and LIDAR (Maltamo et al., 2006). The algorithm used to obtain LiDAR-derived stem maps by NCLFA researchers provided stem detection accuracies of approximately 53% when considering all tree classes at LEF (Suratno et al., 2009). However, stem detection accuracy increases significantly on dominant trees. In similar forest conditions to those of our study area, the stem detection algorithm provided an accuracy of about 90% when considering only dominant trees (Rowell et al., 2006). In this study, we considered only dominant trees with

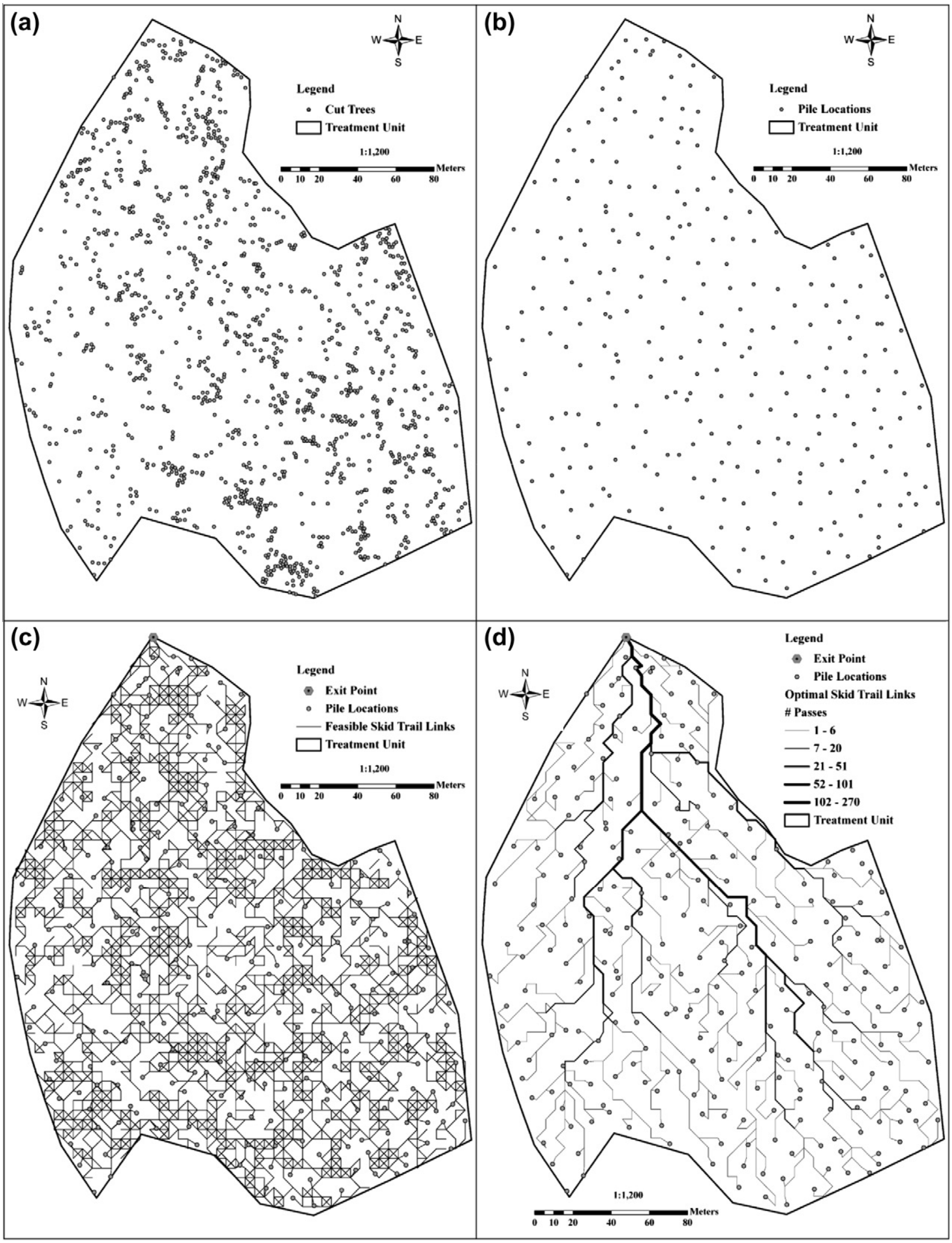

Fig. 9. Cut-tree locations (a) and log-piles (b), feasible skid-trail links (c), and optimal skid-trail network (d) for the selected cut-trees in the best solution found.

DBH > 12.7 cm, thus we expect the stem map used for our study has a high stem detection accuracy level.

Appropriate tree-level growth models are also required to accurately estimate future tree dimensions and consequently tree-level fuel connectivity. We predicted future tree diameters using a basal area increment model parameterized for species commonly found at LEF. However, we assumed that CBH and CW growth proportionally to HT which was derived from DBH. These assumptions may

Table 5
Statistics on individual tree skidding costs estimated for the selected cut-trees in the study area.

Total		Log-piles	
Total skidding cost ($)	3503	Min. number of trees per pile	1.00
Number of log-piles	275	Aver. number of trees per pile	4.52
Number of cut-trees	1265	Max. number of trees per pile	16.00
Harvestable volume (m^3)	36.6	Min. pile volume (m^3)	0.05
		Aver. pile volume (m^3)	1.31
Cut-trees		Max. pile volume (m^3)	2.79
Minimum tree volume (m^3)	0.05	Min. pile distance (m)	14.21
Average tree volume (m^3)	0.29	Aver. pile distance (m)	224.37
Maximum tree volume (m^3)	3.02	Max. pile distance (m)	391.38
Minimum tree cost ($)	0.19	Min. pile cost ($)	6.05
Average tree cost ($)	2.77	Aver. pile cost ($)	12.52
Maximum tree cost ($)	17.27	Max. pile cost ($)	17.27

introduce uncertainty to the accuracy of projected tree sizes and future tree-level fuel connections. Underestimation of future CBH could result in overestimating the number of ignitable trees. Similarly, underestimating future CW could result in underestimation of the number of fuel connections among adjacent pairs of trees.

4. Conclusions

Our computerized approach for optimizing individual tree removal provides an analytical method to evaluate spatial and temporal effects of thinning treatments on reducing crown fire potential within a stand, and thus can help forest managers develop more effective and efficient thinning prescriptions that are site-specific to given stands. Our approach considers spatial variability of fuels within a stand, the effects of cut-tree selection on future tree growth and stand conditions, and skidding costs of individual trees into the development of thinning prescriptions.

Table 6
Comparisons on solution quality between the best tree selection found by the computerized approach and two alternative selections of cut- and leave-trees.

Tree selection method	Objective function value	Skidding cost ($)	Remaining tree-level fuel connections	Future tree-level fuel connections
Computerized model	13,706	3503	4366	5837
Manual	14,327	3483	4548	6296
Random	18,379	3654	6599	8126

The application results show that crown fire potential can be effectively reduced over time while ensuring the cost efficiency of thinning treatments. Fuel connectivity throughout forest stands can be largely reduced in terms of the number of tree-level fuel connections as well as number of clusters of connected trees, average number of trees forming a cluster, and average fuel connections per tree. By selecting the combination of cut-trees that removes the most tree-level fuel connections, our approach can reduce fuel connectivity over time more effectively than commonly used thinning practices. In addition to reducing crown fire potential, our approach can potentially be modified and used for other

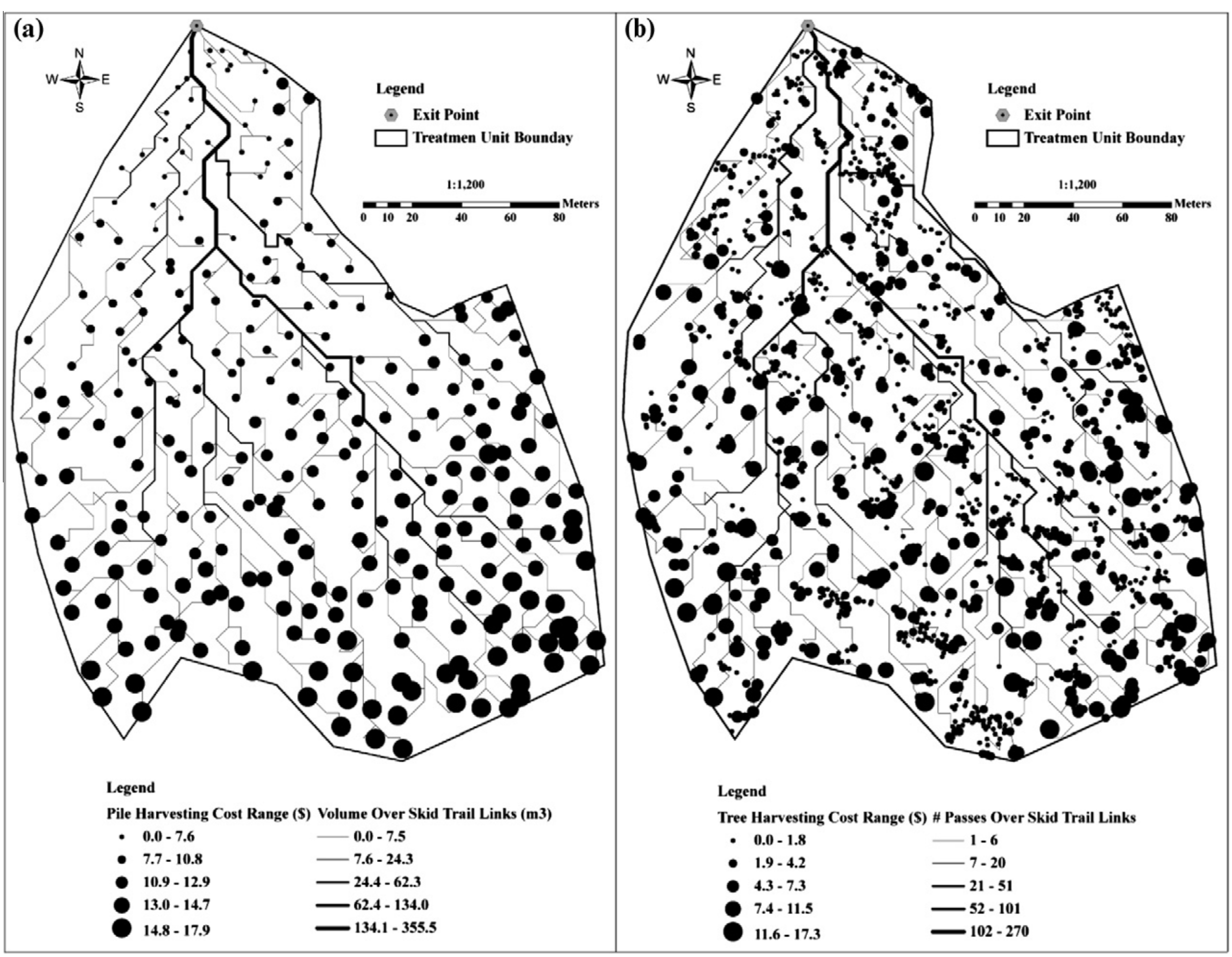

Fig. 10. Distribution of skidding costs over the study area showing cost per log-pile (a) and cost per individual cut-tree (b).

forest management objectives. Tree growth can be included in the objective function to increase timber production as well as reducing crown fire potential. Our approach can also be modified to develop tree-level thinning prescriptions for increasing carbon sequestration or improving wildlife habitat for given species upon availability of tree level measures of carbon sequestration and wildlife habitat quality.

Further research needs to be conducted to enhance the performance of the computerized approach and evaluate the feasibility of implementing the results on the ground. Widely used heuristic optimization techniques such as simulating annealing (Kirkpatrick et al., 1983), tabu search (Glover, 1989, 1990), and ant colony (Dorigo et al., 1996) can be applied to solve the optimal tree removal selection problem and compared with the current random search optimization technique employed in this study. As with all heuristic optimization techniques, solution optimality is not guaranteed. A large number of solutions should then be evaluated to ensure a high-quality solution, although it requires significant computation time. Additional techniques such as parallel programming (Pacheco, 2011) and extreme value theory (Lindgren and Rootzén, 1987; Alvarado et al., 1998) could be implemented into the computerized approach to improve running time and determine the minimum number of solutions required to ensure a desired level of solution quality, respectively.

Despite the imitations, our approach has the potential to enable forest managers to customize site-specific thinning guidelines for individual stands and implement cost-efficient fuel treatments to reduce the risk of high-intensity wildfires. Given that high resolution vegetation mapping technology such as LiDAR is becoming increasingly available, our approach can be a useful tool when thinning is applied to restore overstocked forested lands in need of fuel treatments.

Box 1 Cautionary remark.

In this study we applied the regressions models developed by Contreras et al. (2012) to quantify tree-level fuel connectivity for an entire stand based on the wildland–urban interface Fire Dynamics Simulator (WFDS) as described by Mell et al. (2007). WFDS has received limited field and laboratory evaluation to date as to its validity in simulating surface and crown fire behavior in conifer forest stands. However, the regression models developed by Contreras et al. (2012) were not used to predict tree-level fire behavior per se. Instead they were used as a relative measure to evaluate and compare alternative combinations of cut-trees and select the combination that resulted in the least number of remaining tree-level fuel connections after thinning.

References

Alvarado, E., Sandberg, D.V., Pickford, S.G., 1998. Modeling large forest fires as extreme events. Northwest Sci. 72, 66–75.

Agee, J.K., Skinner, C.N., 2005. Basic principles of forest fuel reduction treatments. For. Ecol. Manage. 211, 83–96.

Anderson, H.E., 1982. Aids to Determining Fuel Models for Estimating Fire Behavior. Gen. Tech. Rep. INT-122. USDA, Forest Service, Intermountain Forest and Range Experiment Station, Ogden, UT, 22p.

Contreras, M., 2010. Spatio-temporal Optimization of Tree Removal to Efficiently Minimize Crown Fire Potential. Ph.D. in Forestry Dissertation, University of Montana, USA, 183p.

Contreras, M.A., Chung, W., 2007. A computer approach to finding an optimal log landing location and analyzing influencing factors for ground-based timber harvesting. Can. J. For. Res. 37, 276–292.

Contreras, M.A., Chung, W., 2011. A modeling approach to estimating skidding costs for individual trees for thinning operations. West. J. Appl. For. 26, 133–146.

Contreras, M.A., Affleck, D., Chung, W., 2011. Evaluating tree competition indices as predictors of basal area increment in western Montana forests. For. Ecol. Manage. 262, 1939–1949.

Contreras, M.A., Parsons, R., Chung, W., 2012. Modeling tree-level fuel connectivity to evaluate the effectiveness of thinning treatments for reducing crown fire potential. For. Ecol. Manage. 264, 134–149.

Daniels, R.C., 2001. Datum conversion issues with LIDAR spot elevation data. Photogramm. Eng. Rem. Sens. 67, 735–740.

Dijkstra, E., 1959. A note on two problems in connexion with graphs. Numer. Math. 1, 269–271.

Dorigo, M., Maniezzo, V., Colorni, A., 1996. The ant system: optimization by a colony of cooperating agents. IEEE Trans. Syst. Cybernet. B 26, 29–41. http://dx.doi.org/10.1109/3477.484436.

Glover, F., 1989. Tabu search – part I. ORSA J. Comput. 1, 190–206.

Glover, F., 1990. Tabu search – part II. ORSA J. Comput. 2, 4–32.

Graetz, D., Sessions, J., Garman, S., 2007. Using stand-level optimization to reduce crown fire hazard. Landsc. Urban Plan. 80, 312–319.

Graham, R.T., Harvey, A.E., Jain, T.B., Tonn, J.R., 1999. The Effects of Thinning and Similar Stand Treatments on fire Behavior in Western Forest. Gen. Tech. Rep. PNW-GTR-463. USDA, Forest Service, Pacific Northwest Research Station, Portland, OR, 27p.

Graham, R.T., McCaffrey, S., Jain, T.B., (Tech. Eds.), 2004. Science Basis for Changing Forest Structure to Modify Wildfire Behavior and Severity. Gen. Tech. Rep. RMRS-GTR-120. USDA, Forest Service, Rocky Mountain Research Station, Fort Collins, CO, 43p.

Hirschmugl, M., Ofner, M., Raggam, J., Schardt, M., 2007. Single tree detection in very high resolution remote sensing data. Rem. Sens. Environ. 110, 533–544.

Lindgren, G., Rootzén, H., 1987. Extreme values: theory and technical applications. Scand. J. Stat. Theory Appl. 14, 241–279.

Keyes, C.R., O'Hara, K.L., 2002. Quantifying stand targets for silvicultural prevention of crown fires. West. J. Appl. For. 17, 101–109.

Keyser, C.E., comp. 2008. Northern Idaho/Inland Empire (NI/IE) Variants Overview – Forest Vegetation Simulator. Internal Rep. USDA, Forest Service, Forest Management Service Center, Fort Collins, CO, 49p (revised February 3, 2010).

Kirkpatrick, S., Gelatt, C.D., Vecchi, M.P., 1983. Optimization by simulated annealing. Science 220, 671–680.

O'Hara, K.L., Seymour, R.S., Tesch, S.D., Guldin, J.M., 1994. Silviculture and our changing profession. J. For. 92, 8–13.

Pacheco, P., 2011. An Introduction to Parallel Programming. Elsevier Inc., 371p.

Maltamo, M., Eerikäinen, K., Packalén, P., Hyyppä, J., 2006. Estimation of stem volume using laser scanning-based canopy height metrics. Forestry 79, 217–229.

Mell, W., Jenkins, M.A., Gould, J., Cheney, P., 2007. A physics-based approach to modelling grassland fires. Int. J. Wildland Fire. 16, 1–22.

Packalén, P., Maltamo, M., 2006. Predicting the plot volume by species using airborne laser scanning and aerial photographs. For. Sci. 52, 611–622.

Popescu, S.C., Wynne, R.H., 2004. Seeing the trees in the forest: using LIDAR and multispectral data fusion with local filtering and variable window size for estimating tree height. Photogramm. Eng. Rem. Sens. 70, 589–604.

Pretzch, H., Biber, P., Dursky, J., 2002. THE single tree-based stand simulator SILVA: construction, application and evaluation. For. Ecol. Manage. 162, 3–21.

Rouvinen, S., Kuuluvainen, T., 1997. Structure and asymmetry of tree crowns in relation to local competition in a natural mature Scot pine forest. Can. J. For. Res. 27, 890–902.

Rowell, E., 2010. Personal Communication. Remote Sensing Analyst. National Center for Landscape Fire Analysis, College of Forestry and Conservation, University of Montana, Missoula, MT.

Rowell, E., Seielstad, C., Vierling, L., Queen, L., Shepperd, W., 2006. Using laser altimetry-based segmentation to refine automated tree identification in managed forests of the Black Hills, South Dakota. Photogramm. Eng. Rem. Sens. 72, 1379–1388.

Rowell, E., Seielstad, C., Goodburn, J., Queen, L., 2009. Estimating plot-scale biomass in a western North American mixed-conifer forest from lidar-derived tree stems. In: Silvilaser 2009. Proceedings of the 9th International Conference on Lidar Applications for Assessing Forest Ecosystems, Texas A&M University, October 15, 2009.

Schmidt, K.M., Menakis, J.P., Hardy, C.C., Hann, W.J., Bunnell, D.L., 2002. Development of Coarse-Scale Spatial Data for Wildland Fire and Fuel Management. Gen. Tech. Rep. RMRS-GTR-87. USDA, Forest Service, Rocky Mountain Research Station, Fort Collins, CO, 41p.

Scott, J.H., Reinhardt, E.D., 2001. Assessing Crown Fire Potential by Linking Models of Surface and Crown Fire Behavior. Res. Pap. RMRS-RP-29. USDA, Forest Service, Rocky Mountain Research Station, Fort Collins, CO, 59p.

Skov, K.R., Kolb, T.E., Wallin, K.F., 2004. Tree size and drought affect ponderosa pine physiological response to thinning and burning treatments. For. Sci. 50, 91.
Suratno, A., Seielstad, C., Queen, L., 2009. Tree species identification in mixed coniferous forest using laser scanning. ISPRS J. Photogramm. Rem. Sens. 64, 683–693.
Terrasolid, 2004. TerraScan User's Guide. Helsinki.
USDA, Forest Service, and USDI, Bureau of Land Management, 2001. The National Fire Plan: Managing the Impacts of Wildfires on the Communities and the Environment. <http://www.forestsandrangelands.gov/>.